REVIEW

Magnetic iron oxide nanogels for combined hyperthermia and drug delivery for cancer treatment

Sofia Patri, [ID] [a] Nguyen Thi Kim Thanh [ID] *[b,c] and Nazila Kamaly [ID] *[d]

Hyperthermia and chemotherapy represent potential modalities for cancer treatments. However, hyperthermia can be invasive, while chemotherapy drugs often have severe side effects. Recent clinical investigations have underscored the potential synergistic efficacy of combining hyperthermia with chemotherapy, leading to enhanced cancer cell killing. In this context, magnetic iron oxide nanogels have emerged as promising candidates as they can integrate superparamagnetic iron oxide nanoparticles (IONPs), providing the requisite magnetism for magnetic hyperthermia, with the nanogel scaffold facilitating smart drug delivery. This review provides an overview of the synthetic methodologies employed in fabricating magnetic nanogels. Key properties and designs of these nanogels are discussed and challenges for their translation to the clinic and the market are summarised.

1. Introduction

Conventional treatments for cancer, such as chemotherapy and radiotherapy,[1] while essential, are often accompanied by profound and debilitating side effects. These unwanted reactions, alongside the emergence of drug resistance, highlight the need for innovative therapeutic approaches.[2]

In response, combinatorial approaches have emerged for cancer treatment over the years.[3] Therapies such as photodynamic or ultraviolet light therapy have shown the potential to weaken cancer before chemotherapy.[3] Notably, the rise of combinatorial therapy can be traced to the convergence of nanotechnology and cancer therapeutics. This has enabled the development of precision-engineered therapies with superior targeting capabilities, reduced systemic toxicity, and promising clinical outcomes.[4]

This review focuses on the combination of magnetic hyperthermia and chemotherapy with the use of magnetic iron oxide nanogels.

Hyperthermia and chemotherapy are established modalities in cancer treatment, each with distinct drawbacks.[5] While hyperthermia poses risks of invasiveness and adverse effects

such as heat-related complications including heat strokes, heat cramps, and dehydration,[6] chemotherapy often inflicts severe side effects on patients due to medication toxicity. Combining the two therapies offers the advantage of localised heat and lower drug doses, as the treatment can leverage both the cytotoxic effects of the drugs and the hyperthermic action, thus enhancing therapeutic efficacy while potentially mitigating the individual drawbacks associated with each modality.

2. Magnetic hyperthermia

Hyperthermia therapy relies on the thermal effects on cancer cells.[7] The susceptibility of cancer cells to heat-induced damage was demonstrated in pioneering research done by Woodhall *et al.* in the 1960s.[8] At temperatures around 43 °C and in the absence of hyperthermia-enhancing agents, the vasculature of tumour tissues, characterised by abnormalities, experiences a notable reduction in blood flow. This reduction impairs the delivery of oxygen and nutrient supplies to the tumour cells, leading to cell death.[7] At the same temperature, healthy cells exhibit resilience to thermal stress.

Diverse approaches to hyperthermia treatment are employed based on tumour characteristics such as location and size. For instance, whole-body hyperthermia techniques such as hot baths or saunas are utilised for extensive skin tumours. These techniques elevate the patient's temperature up to the tolerance limit, typically around 41 °C.[9] For deep-seated tumours, localised heat application is achieved through the use of metal probes.[10] In recent years, the field has wit-

[a]Department of Materials, Molecular Sciences Research Hub, Imperial College London, 82 Wood Ln, London W12 0BZ, UK. E-mail: sofia.patri18@imperial.ac.uk
[b]UCL Healthcare Biomagnetic and Nanomaterials Laboratories, 21 Albemarle Street, London W1S 4BS, UK. E-mail: ntk.thanh@ucl.ac.uk; https://www.ntk-thanh.co.uk
[c]Biophysic Group, Department of Physics and Astronomy, University College London, London WC1E 6BT, UK
[d]Department of Chemistry, Molecular Sciences Research Hub, Imperial College London, 82 Wood Ln, London W12 0BZ, UK. E-mail: nazila.kamaly@imperial.ac.uk

nessed a shift towards less invasive yet highly efficient methods such as magnetic hyperthermia (MH).

Magnetic hyperthermia harnesses the heat-generating potential of magnetic nanoparticles (NPs) when exposed to alternating magnetic fields (AMFs).[11] This technique offers significant advantages, notably the ability of AMFs to penetrate tissues deeply and the option to directly administer nanoparticles into the tumour site, rendering the therapy minimally invasive,[11] Fig. 1.

2.1 Iron oxide nanoparticles

Iron oxide nanoparticles (IONPs) are one of the few magnetic nanoparticles approved by the FDA for biomedical applications.[10] They are made of magnetite (Fe_3O_4) or maghemite (γ-Fe_2O_3) with an inverse spinel structure.[12] IONPs are non-toxic and undergo metabolisation primarily by the spleen and liver;[13] the iron component holds potential for utilisation in haemoglobin production.[14]

Sofia Patri

Sofia graduated from Imperial College London with a first class honours MSci in Chemistry in 2022. During her master, Sofia worked on small pyridine macrocycles for rotaxane formation under the supervision of Dr Jamie Lewis. Sofia's research interests is in nanomedicine, particularly in novel targeted magnetic therapies for simultaneous drug delivery and hyperthermia therapy. Sofia is now a PhD student studying in the Centre of Doctoral Training in Advanced Characterisation of Materials, under the supervision of Dr Nazila Kamaly at Imperial College and Prof. Nguyen Thi Kim Thanh at UCL.

Nguyen Thi Kim Thanh

Professor Nguyen Thi Kim Thanh, MAE, FRSC, FInstP, FAPS, FIMMM FRSB (https:// www.ntk-thanh.co.uk) held a prestigious Royal Society University Research Fellowship (2005–2014). She was appointed a Full Professor in Nanomaterials in 2013 at University College London. She leads a very dynamic group conducting cutting edge interdisciplinary and innovative research on the design, and synthesis of magnetic and plasmonic nanomaterials mainly for biomedical applications. In 2019, she has been honoured for her achievements in the field of nanomaterials, and was awarded highly prestigious Royal Society Rosalind Franklin Medal. She was RSC Interdisciplinary Prize winner in 2022. She was awarded SCI/RSC Colloids Groups 2023 Graham Prize Lectureship to recognise an outstanding mid-career researcher in colloid and interface science. She is one of only 12 recipients globally of 2023 Distinguished Women in Chemistry/Chemical Engineering Awards, bestowed by the International Union of Pure and Applied Chemistry (IUPAC). Currently, she is Vice Dean for Innovation and Enterprise at Faculty of Maths and Physical Sciences. She was elected as a member of Academia Europaea in April 2024. She is Editor-in-chief of the Royal Society of Chemistry book Series, Nanoscience and Nanotechnology and an Associate Editor for Nanoscale and Nanoscale Advances Journals. She edited 7 theme issues including: Design and scaling up of theranostic nanoplatforms for health: towards translational studies. Nanoscale, RSC (2023); Theranostic nanoplatforms for biomedicine Nanoscale, RSC (2021); Multifunctional nanostructures for diagnosis and therapy of diseases. Interface Focus, The Royal Society (2016); Volume 175: Physical Chemistry of Functionalised Biomedical Nanoparticles. Faraday Discussions, RSC (2014); Special issue: Functional Nanoparticles for Biomedical Applications. Nanoscale, RSC (2013); Nanoparticles Theme, Philosophical Transactions of the Royal Society A, The Royal Society (2010). She is the sole editor of two seminal books on Magnetic Nanoparticles from Fabrication to Clinical Applications (https://tinyurl.com/ y5bgxb3r) and Clinical Applications of Magnetic nanoparticles (https://tinyurl.com/yyjawnz2).
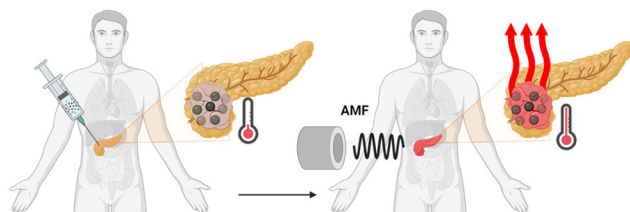
Fig. 1 Magnetic hyperthermia due to injected nanoparticles interacting with AMF (created with BioRender.com).

Both the biocompatibility and performance of IONPs are strictly related to the magnetic properties of the NP. The properties, in turn, depend on the size, crystallinity, and purity of the material.[12] The ideal properties for MH are obtained with mono-dispersed and colloidally stable IONPs. This can be achieved with several synthetic strategies, such as alkaline precipitation of iron salts in water,[15,16] thermal decomposition,[17] polyol mediated synthesis[18] and lithography.[19]

2.1.1 Magnetic properties of IONPs. The magnetism exhibited by IONPs originates from the magnetic field induced by the spin–orbit coupling of the electrons. This coupling describes the interaction of the electron movement with its spin.[12]

When IONPs are subjected to an external magnetic field or AMF, the electron spins orient themselves along the direction of the applied field;[20] once all the spins are aligned, the material reaches magnetisation saturation (M_S), represented as a plateau in magnetisation curves,[21] Fig. 2. These curves are obtained by measuring the magnetisations of the sample under different magnetic field strengths.[12]

As the AMF is removed, the material will retain some residual magnetisation (M_R), resulting in a hysteresis loop.[12] The remanent magnetisation is one of the causes of particles' aggregation, which can lead to clot formation in the arteries.[12] The magnetisation curves and M_S values are significantly influenced by the size and morphology of the particles.[22] Consequently, IONPs may display varying M_S values depending on the synthetic method, batch, and degree of polydispersity. Only recently, LaGrow et al. provided a solution for the reproducible synthesis of IONP. By investigating the growth mechanism of the co-precipitation synthesis method with the aid of synchrotron X-ray diffraction in solution,[23] they were able to provide a comprehensive understanding of the mechanism. This is essential not only for robust syntheses, but also for greater control over the size of the iron oxide nanoparticles, and hence the tuning of their magnetic properties.

At diameters below 25 nm, the energy needed for spin reorientation falls below the thermal energy barrier.[12] Consequently, IONPs of this size range do not retain residual magnetisation upon removal of the AMF. Instead, excess magnetic energy dissipates into the surroundings as heat through the physical motion of particles (Brownian relaxation) or the rotational movement of magnetic moments (Néel relaxation).[12] Materials with this characteristic are called superparamagnetic;[12] this property is essential in biological applications as it prevents the aggregation of the particles.[12]

The magnetic field frequencies employed in MH therapy are considered safe for human health. The bottleneck when using the IONPs is that there is not enough heat generated and a high dose of IONPs is required.[24] Therefore, researchers are focusing on enhancing the heating efficiency of IONPs to minimise the required quantity for treatment.

Nazila Kamaly

Dr Nazila Kamaly is a Senior Lecturer in the Department of Chemistry at Imperial College London. She received her MSci degree in Medicinal Chemistry from University College London and completed her PhD in the Chemistry Department at Imperial College London. Following her doctoral studies, Dr Kamaly held Postdoctoral and Instructor positions at Massachusetts Institute of Technology (MIT) and Harvard Medical School from 2011 to 2016. Prior to joining Imperial College London, Dr Kamaly was an Associate Professor at the Technical University of Denmark, where she was awarded a Lundbeck Fellowship to develop targeted nanomedicines for the treatment of heart disease. Dr Kamaly leads a multidisciplinary research group that focuses on developing bioinspired approaches for the synthesis of bottom-up multifunctional polymeric nanoparticles and biomaterials. These novel materials are designed to respond to local or up-regulated disease markers, enabling stimuli-responsive and spatiotemporally controlled drug delivery. Additionally, her group investigates the nanoparticle-biointerface using biomicrofluidic models with controlled environmental parameters to develop innovative biomimetic drug delivery routes and assess nanoparticle physicochemical properties.

Fig. 2 Magnetisation curve and hysteresis loop of a ferromagnetic and a superparamagnetic material. The curves show the magnetisation saturation (MS), the retentivity (HR) and the coercivity (HC) (created with BioRender.com).

The heating efficiency of IONPs is quantified in terms of specific power absorption (SAR), representing the energy released per unit mass.[17] A SAR of 300 W g^{-1} with a magnetic field of frequency and amplitude of 100 kHz and 10 kA m^{-1} respectively is appropriate for hyperthermia applications in humans.[25,26]

This could be achieved with 4 mL of magnetic fluid with a concentration of 120 mg mL^{-1}, assuming a homogeneous distribution of the NPs inside a tumour with volume of 20 mL and no losses outside the tumour site.[26] It is important to note that the SAR diminishes with increased tumour volumes; this highlights the importance of a precisely targeted delivery of the NPs inside the tumour.[27] Commercially available IONPs can only reach 100 W g^{-1}.[28] It should be noted that the SAR depends on the IONP properties and the AMF amplitude and frequency.[29]

In 2013, Meffre *et al.* synthesised a series of core–shell iron/iron carbide nanoparticles with a SAR of 415 W g^{-1} in a magnetic field with a frequency of 54 kHz and amplitude of 24 kA m^{-1}.[30]

In 2014, Di Corato *et al.* tested the SAR of several magnetic nanomaterials in solution and the cellular environment.[31] Having tested single round particles, agglomerations and cubes, they reported heating up to 42 °C in a field with a frequency of up to 700 kHz and amplitude of up to 24 kA m^{-1}. Notably, all tested nanomaterials exhibited a decrease in SAR upon cellular internalisation,[31] demonstrating the influence of environmental factors on SAR.[17] To achieve a SAR of approximately 300 W g^{-1} (ref. 27) in the cellular environment, the IONPs should have exceptionally high SAR in solution. For more information on magnetic hyperthermia, and its relation with IONP properties and the environment, we refer the reader to publications elsewhere.[31–39]

To summarise, the ideal IONPs for hyperthermic applications should possess the following characteristics:

• Composition: they are composed of magnetite (Fe$_3$O$_4$) or maghemite (γ-Fe$_2$O$_3$) with an inverse spinel structure.[12]

• Size: Their diameter should be less than 25 nm to exhibit superparamagnetic properties.[40]

• Specific absorption rate (SAR): they should ideally exhibit a SAR value of approximately 300 W g^{-1} (ref. 27) under a magnetic field frequency of 100 kHz and an amplitude of 10 kA m^{-1}.[30]

2.1.2 Colloidal stability of IONPs. In 2017, Stocke *et al.* performed MH using IONPs on mice affected by lung cancer, demonstrating a significant reduction in tumour growth.[24] Initial results indicated that optimal efficacy was achieved with high doses of IONPs.[24] However, high doses of IONPs can pose several potential problems, primarily related to their cytotoxicity and interactions within biological systems. Several reviews in the literature report an overview of the toxicology, distribution, clearance, pharmacokinetics of IONPS and hydroxyl radical formation *via* Fenton reaction.[4,41–50] Here, we will focus on the systemic danger associated with the IONPs aggregation.

The tendency of IONPs to aggregate, driven by factors such as van der Waal forces, poses potential risks of pulmonary embolism or coagulation.[51] This can be counteracted by covering the IONPs in an organic coating. The coating provides steric and electrostatic repulsion while enhancing the colloidal stability and the biocompatibility of the metal oxide particles.[51] In 2015, Walter *et al.* functionalised the surface of IONPs with PEGylated mono-phosphonated dendrons.[52] Their investigation revealed that the conical architecture of the dendron contributes to the enhanced colloidal stability of the IONPs, attributed to the introduction of steric hindrance.[52] Additionally, polymeric coatings like chitosan offer a means to increase the repulsive forces between the IONPs.[53]

Furthermore, employing a soft coating material enables IONPs to serve as a drug delivery system (DDS), facilitating combination therapy with other treatments.[54–57] While hyperthermia alone may not suffice for complete cancer eradication, it can synergise with drug interventions by weakening cancer cells.[7,11]

2.1.3 Polymer coatings for IONPs. Various organic nanoparticles and nanoplatforms have been employed in literature to encapsulate IONPs for biomedical applications, as summarised in Table 1. These are also graphically shown in Fig. 3.

Dendrimers are 3D macromolecules, comprising an inner core and branching outer layers.[58] Such dendrimer-covered IONPs are often used in magnetic resonance imaging (MRI) as dendrimers can facilitate the penetration of IONPs inside cells.[59]

Micelles, colloidal dispersions of amphiphilic molecules arranged in a particle-like shape,[60] also aid in cellular uptake of IONPs for imaging purposes.[61]

Microbubbles are spherical polymeric structures containing a gas core.[62] By encapsulating IONPs in microbubbles, the IONPs can be delivered inside the cells by sonoporation.[62]

Polymers, such as polyethylene glycol (PEG), can be grafted on the surface of IONPs to prolong their circulation time.[63] Additionally, polymers can also impart controlled drug delivery properties to IONPs: for example, Zhang *et al.* coated their IONPs with poly(*N*-isopropylacrylamide) (PNIPAAM) to facilitate the development of a magnetic DDS with thermo-responsive characteristics.[64]

Liposomes, hollow spherical particles composed of a lipid bilayer,[12] exhibit less stability compared to other platforms, leading to potential leakage of contents over time.[1]

Hydrogels are formed by polymer chains crosslinked to give a 3D network with a highly porous nature that encapsulates water.[12] Similar to liposomes, hydrogels are highly biocompatible but they excel in shielding the payload from degradation.[12]

From Table 1, it can be noted that polymers, liposomes and hydrogels are the most extensively studied for drug delivery.

3. Localised delivery of chemotherapy drugs with nanogels

Chemotherapy relies on small-molecule antiplastic drugs to either kill cancer cells or inhibit their growth.[74] These drugs suffer from short circulation half-lives and poor water solubi-

Table 1 Nanoplatforms for encapsulating magnetic nanoparticles and their applications

Platform	Size	Shape and structure	MNP hybridisation method	Applications	Ref.
Dendrimers	7–11 nm	MNPs covered in dendrimers	*In situ* MNP synthesis	MRI imaging	59 and 65
Polymers	10 to 100 nm	Single MNP with a polymer shell	*In situ* MNP synthesis grafting	Drug delivery, MRI imaging, hyperthermia	56, 57, 63, 64 and 66
Liposomes	>100 nm	MNPs embedded in lipid bilayer	Formation of liposomes in in presence of pre-formed MNP	MRI imaging, drug release, hyperthermia	67–69
Micelles	40 to 135 nm	IONPs encapsulated in micelles	Grafting in presence of water to induce micelles	MRI imaging	61
Microbubbles	1–4 μm	Gas core, shell of polymer and MNP	Pre-formed MNP distributed in polymer layer during synthesis	MRI imaging, drug delivery	55 and 62
Hydrogel	300 nm– 150 μm	Hydrogel shell with IONPs core	*In situ*, blending, grafting	Drug delivery, hyperthermia	70–73
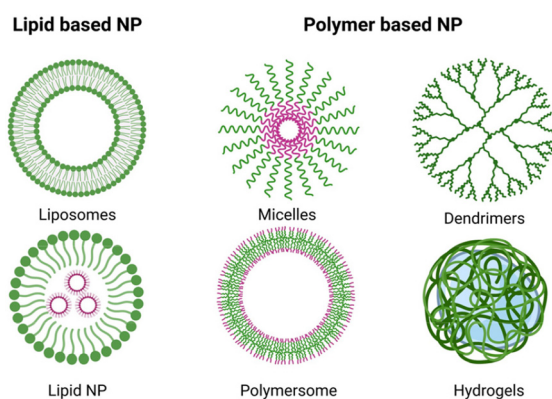
Fig. 3 Types of nanoparticles for drug delivery (created with BioRender.com).
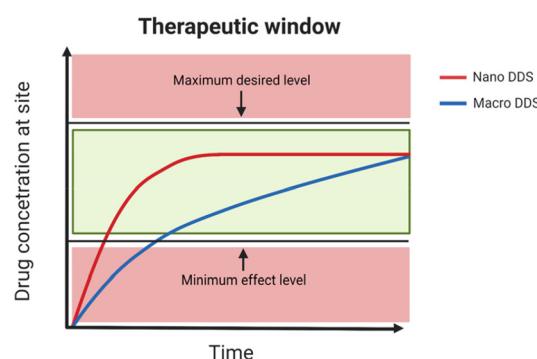
Fig. 4 The therapeutic window for an ideal nano-sized DDS and a macro DDS (created with BioRender.com).

lity,[1] hindering their ability to reach the tumour site. Higher doses are typically administered to patients to ensure therapeutic efficacy, albeit at the cost of impacting healthy cells in the body.

In recent years, these shortcomings have been addressed with the development of biomaterial carriers, DDS.[4] The DDS platforms shield the drugs from the biological environment, extending their circulation time, and offering precise control over drug release kinetics and localisation through external manipulation.[1] The main aim of a DDS is to enhance the therapeutic window of the drug. As Fig. 4 shows, nano-sized DDS facilitate a more uniform release of the drug over time, achieving the minimum effective level earlier than macro-sized DDS.[75]

The design of an efficient nano-carrier should address the following points:[75]

• Encapsulation: The nanocarrier must exhibit high encapsulation efficiency to minimise the dosage required for therapy. Additionally, the carrier's shell should effectively prevent cargo leakage before the intended release.[75]

• Stimuli-response: the release of the cargo should be controlled by a stimulus to prevent premature release.[76]

• Passive targeting: the size and morphology should be tailored to target the tumour thanks to the enhanced permeability and retention effect (EPR). EPR is caused by the abnormal growth of the tumour's vasculature and the poorly formed lymphatic systems.[76]

• Active targeting: Incorporating ligands capable of targeting specific receptors expressed by tumour cells enhances the accumulation of DDS within the tumour site.[75]

• Ease of synthesis: the synthesis of the nanocarrier should be scalable for commercialisation and the post-processing should be straightforward and time-effective.

Hydrogels and liposomes can both be engineered to meet the criteria for an ideal drug delivery system. However, hydrogels are more suitable for combined hyperthermia and chemotherapy applications due to their three-dimensional polymer network, which effectively prevents the leakage of IONPs over time.[1] For other systems capable of simultaneous hyperthermia and drug delivery, the reader is invited to read the review by Hervault *et al.*[21]

3.1 Nanogels

As shown in Table 1, hydrogels incorporating IONPs may possess larger diameters that could impede biomedical applications.[4] To optimise functionality, hydrogels must be sized appropriately to evade antibody interference [4] and traverse biological barriers for intracellular drug delivery.[76] The nano-range size can be achieved by constraining the diameter of the hydrogels to the nano-scale (<500 nm), rendering them as

nanogels. The size constraint can be achieved *via* traditional microemulsion polymerisations[75] or more recent strategies such as micro-moulding and micro-fluidic methods.[77] A diverse array of natural and synthetic polymers can be used to form nanogels[78] with good biocompatibility; for biomedical applications, natural or FDA-approved polymers, such as PEG, are preferred.[79]

Nanogels can undergo crosslinking through either physical interactions or covalent chemical bonds.[79] Physically crosslinked nanogels are synthesised in mild conditions and are less likely to carry toxic contaminants, such as unreacted monomers or catalysts.[79] However, these nanogels are also less stable in physiological conditions and it is more difficult to control the cargo release.

Chemically crosslinked nanogels are given by a bonding reaction between the chains of the polymers. These nanogels exhibit enhanced stability and are better suited for biomedical applications.[79] Many cross-linking reactions can be used to form chemically crosslinked nanogels, such as radical polymerisation,[80] click chemistry and copper-free click chemistry,[81,82] amide crosslinking[83] or photocrosslinking.[84]

3.1.1 Properties of nanogels for drug delivery. Nanogels are excellent drug carriers thanks to their porous nature.[76] They can incorporate a large number of drugs thanks to their extensive inner surface area and the ability to coordinate the payload with their functional groups.[79] There are three main mechanisms for the incorporation of drugs, Fig. 5:

• **Physical entrapment**: drugs are entrapped by mixing them with pre-formed nanogel;[85]

• **Covalent conjugation**: drugs form covalent bonds with nanogels *via* pendant functional groups on polymer chains or the backbone.[86] The disruption of these covalent bonds is necessary for drug release into the environment;[87]

• **Self-assembly**: electrostatic interactions or hydrophobic interactions facilitate drug coordination with polymer chains.[88]

Upon reaching the target site, drug release from the nanogel is regulated by the mesh size of the network. The mesh size is influenced by crosslinking points and polymer nature.[89] If the drug cannot freely travel outside of the network by diffusion, several strategies allow for a more controlled release, such as degradation, which permanently disrupts the 3D network of the gel.[90]

Alternatively, the nanogel can be forced to undergo an induced transition. For example, the network can be shrunk, leading to water and cargo expulsion.[76] Nanogels capable of such trigger-induced changes are termed stimuli-responsive, exhibiting reversible alterations in conformation or solubility,[76] Fig. 6.

For combined magnetic hyperthermia and chemotherapy, the conformational change of the nanogel should be triggered by a rise in temperature, induced by the IONPs.[11] The ability of the nanogel to swell or shrink is governed by a volume phase transition known as coil-to-globule transition,[91] Fig. 7.
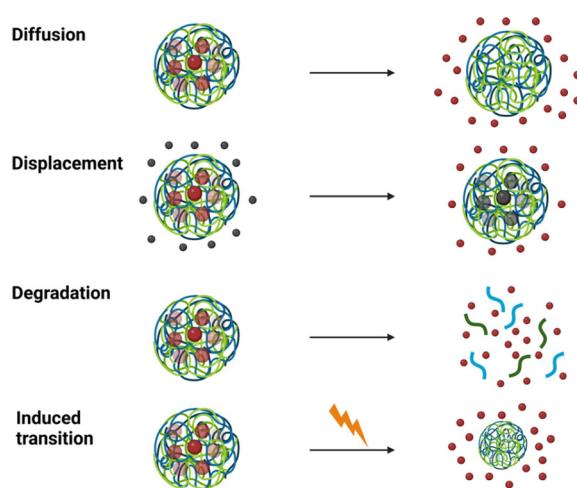
Fig. 6 The main mechanisms of drug release from nanogels (created with BioRender.com).


Fig. 5 The main mechanisms of drug loading in nanogels (created with BioRender.com).
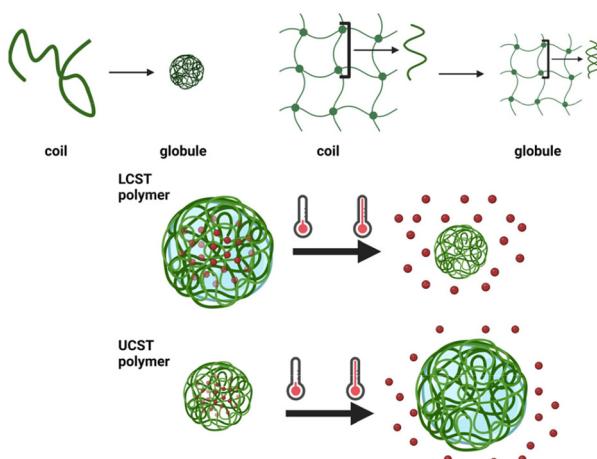

Fig. 7 Coil to globule transition in polymer chains and nanogels; LCST and UCST polymers (created with BioRender.com).

In a polymer solution, above a certain temperature known as the lower critical solution temperature (LCST), the entropy penalty becomes prohibitive to maintain the coil configuration. The penalty prompts the polymer chain to collapse onto itself to shield the hydrophobic sections from solvent molecules, forming a globule.[92] The transition is governed by the ratio between the hydrophobic and hydrophilic units in the polymer.[92]

In a nanogel, the coil-to-globule transition results in the shrinking of the network with the expulsion of the solvent from the mesh;[91] some nanogels can undergo the opposite transition, from a collapsed to a swollen state, upon reaching an upper critical solution temperature (UCST).[93]

Nanogels undergo this structural change faster than hydrogels as the time to achieve this transition is proportional to the square of their length.[91]

Thermoresponsiveness is given by a thermosensitive unit in the nanogel formulation, such as PNIPAAM, LCST = 32 °C (ref. 79) or poly(N-vinylcaprolactam) (PVCL, LCST = 32 °C).[95] As the ideal temperature for hyperthermia is above 40 °C,[57] as demonstrated by Wang et al.: at 40 °C, around 50% of the cancer cells died under exposure to AMF. Hence, the nanogel should be engineered to exhibit a sharp transition at this temperature.

One strategy to raise or lower the LCST of the polymer is through copolymerisation of more hydrophilic or hydrophobic monomers. By adjusting the ratio of these monomers, the desired temperature range can be achieved.[96,97] However, the addition of monomers to lower the LCST often results in a broadening of the transition temperature range, complicating control.

Alternatively, the addition of branching units or the variation of the chain length has also demonstrated efficacy in altering the LCST,[93,98] Fig. 8.

Overall, the ideal nanogel formulation for combined hyperthermia and drug delivery should possess the following properties:

• Composition: it should be composed of FDA-approved or biocompatible polymers, such as PEG.

• Drug release: the nanogel should release its cargo in response to an external stimulus, specifically heat.
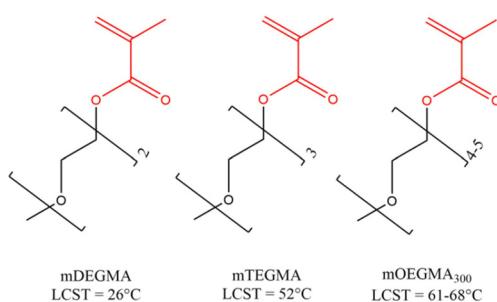
• Thermo-responsivity: it should demonstrate a distinct phase transition temperature in the range of 40–45 °C.[57]

4. Combinatorial therapies

While DDSs have demonstrated efficacy in mitigating chemotherapy toxicity, addressing the adaptability of tumours and achieving complete eradication of malignant growths necessitates the development of multifunctional therapies.[74]

Petryk et al. showed that, following heat treatment, cancer cells exhibit reduced drug resistance, rendering synergistic therapy 1.5 times more effective than chemotherapy alone.[99] Similar results have been reported by Wang et al.[57] A Phase III clinical trial report highlighted that the combination of hyperthermia and chemotherapy doubled the life expectancy of patients with soft tissue sarcoma.[5] Fig. 9 shows a graphical representation of the simultaneous action of hyperthermia and chemotherapy.

To effectively combine these two different therapies, it is necessary to understand the properties of each material, how to enhance them in the therapy, and how they are affected by the biological environment.[1]

In the sections below, the synthesis, properties and applications of iron oxide magnetic nanogels will be covered.

5. Synthesis of magnetic nanogels

The magnetic nanogels reviewed in this study feature IONPs encapsulated within a nanogel shell. Different structures have been reported in the literature, all of which depend on the synthesis method of the magnetic nanogels.

5.1 Synthesis by physical entrapment

The blending and in situ are two prominent techniques relying on the physical entrapment of IONPs within the nanogel structure. Both methods have been extensively used since the early 2000s for magnetic hydrogel/nanogel synthesis,[100–105] Fig. 10.

In the blending method, non-covalent interactions are commonly used to form stable intermediates; a subsequent crosslinking reaction forms the magnetic nanogels. Vijayan et al. achieved pre-organisation of the magnetic nanogel structure through electrostatic interactions between negatively charged citric acid-coated IONPs and the positively charged 2-(dimethylamino)ethyl methacrylate.[102] Following the crosslinking

Fig. 8 Non-linear PEG derivates and their LCST.[94] mDEGMA – di(ethylene glycol) methyl ether methacrylate; mTEGMA – tri(ethylene glycol) methacrylate; mOEGMA – oligo(ethylene glycol) methyl ether methacrylate.

mDEGMA LCST = 26°C
mTEGMA LCST = 52°C
mOEGMA$_{300}$ LCST = 61-68°C
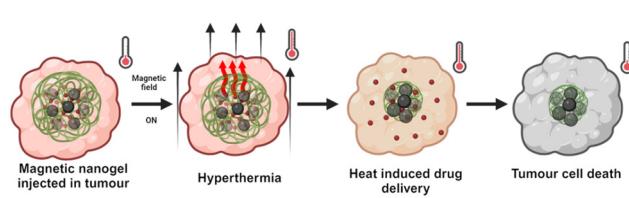
Fig. 9 Representation of simultaneous hyperthermia and drug delivery (created with BioRender.com).

Magnetic nanogel injected in tumour — Hyperthermia — Heat induced drug delivery — Tumour cell death
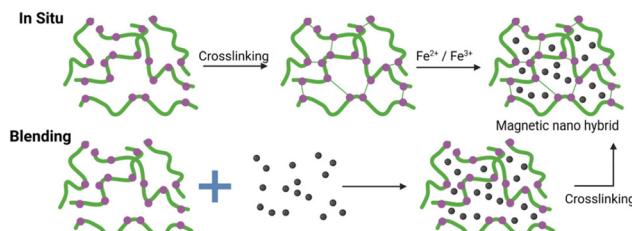
Fig. 10 Pictorial representation of the blending and *in situ* methods (created with BioRender.com).

reaction, a negatively charged, 80 nm spherical magnetic nanogel was formed, even if only 2.5 wt% of IONPs were incorporated in the nanogel.

In 2013, Chiu and co-workers synthesised hollow hybrid nanogels by photoinitiated polymerisation of a nanogel in the presence of citric acid-coated IONPs.[106] They exploited the temporary hydrogen bonding (H-bond) of the citric acid and the PNIPAAM grafts of the nanogel precursor to form an assembly at pH 3 with a diameter of 198 nm. Covalent cross-linking of polymer chains was subsequently executed to secure a stable system with a diameter of 208 nm even at higher pH. Remarkably, approximately 44 wt% of IONPs were incorporated into the nanogels, rivalling previous literature records.[106] However, the *blending* method offers limited control over IONP incorporation into the matrix, potentially altering predicted properties and leading to unwanted aggregate formation.[103] In the study by Chiu and co-workers, the M_S of the IONPs synthesised decreased from 77 emu g^{-1} to 36 emu g^{-1} post-polymerisation.[106]

The *in situ* method provides a simpler synthetic approach by utilising the micro/nanogel as a microreactor. But, as with the *blending* method, controlling the morphology and consequently the properties of magnetic nanogels remains challenging.[103]

The absence of a strong bond between the IONPs and the nanogel chains can lead to a leakage of the IONPs over time. Such leakage not only undermines the functionality of the composite, as the IONPs can no longer facilitate drug delivery, but it also poses potential toxicity concerns.[107,108] By introducing a covalent bond between the IONPs and the nanogel, the composites can be constructed in a "bottom-up" fashion with higher control over the structure.[109]

5.2 Synthesis by covalent grafting

The grafting approaches rely on the use of ligands featuring functional groups capable of binding with the surface, Fig. 11. These ligands commonly include carboxylic acids,[51,110] tri-methoxysilanes,[17] and phosphonic acids.[111,112] A key attribute of these bonds is their capacity to withstand high temperatures, a crucial requirement for hyperthermia applications.[109]

5.2.1 Grafting to. In the *grafting to* approach, the binding group is located at the end of the polymer chain to anchor the pre-formed polymer to the IONP surface.[109] This can be
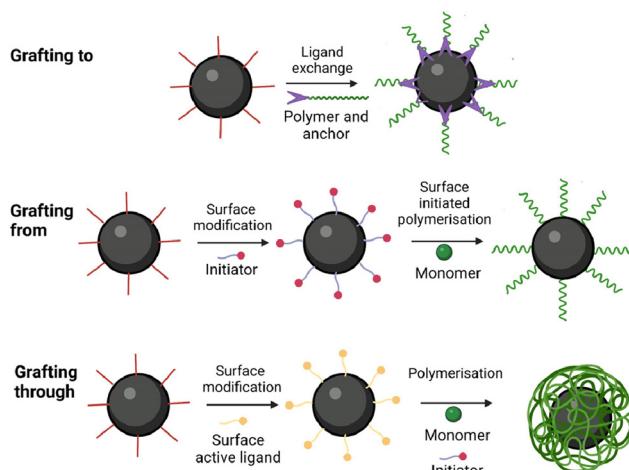

Fig. 11 Pictorial representation of the grafting methods (created with BioRender.com).

accomplished using bare IONPs or *via* ligand exchange with the coating of the IONPs.

Cazares-Cortes *et al.* synthesised MagNanogels by incorporating the IONPs at pH 3 utilising their positive surface charge for easy diffusion through the neutral polymer matrix.[113] By increasing the pH to 7, the IONPs are neutralised and carboxylic functionalities of the nanogel can bind to the surface of the IONPs. This approach, previously used by Boularas *et al.*,[114] resulted in a homogeneous distribution of IONPs throughout the polymer matrix without aggregation, Fig. 12. However, the MagNanogels were found to be stable only up to a wt of 37.5% iron content. Those with wt percentages of 50 and 66.7% exhibited instability due to the presence of aggregates on the surface.[113]

5.2.2 Grafting from. In the *grafting from* approach, the initiator for the nanogel polymerisation is incorporated into the surface ligand. Kurzhals *et al.* conducted a comparative study of the *grafting from* and the *grafting to* methods by pre-
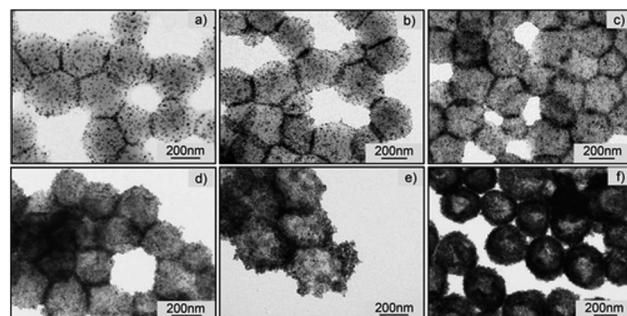
Fig. 12 Transmission electron microscopy (TEM) images of the MagNanogels synthesised by Cazares-Cortes *et al.* with different IONPs content (from (a) to (f): 9.0, 16.7, 28.6, 37.5, 50.0, and 66.7 wt%).[113] Reprinted with permission from E. Cazares-Cortes *et al.*, *ACS Appl. Mater. Interfaces*, 2017, **9**(31), 25775–25788. Copyright 2017 American Chemical Society.

paring the same magnetic hydrogel:[109] the *grafting from* approach resulted in a denser polymeric coating compared to the *grafting to* method. In the *grafting to* method, the structural arrangement of the polymer chains obstructed the access of IONPs surfaces to other polymers, thus limiting the coating density. However, the magnetic nanogel formed by the *grafting from* approach exhibited unwanted and uncontrolled clustering of the cores due to challenges in dispersing the initiator-coated IONPs in water.[109]

5.2.3 Grafting through. The *grafting through* method involves the anchoring of surface active monomers. These monomers have a functionality, such as a vinyl group, capable of participating in the polymerisation. Through this process, the IONPs are incorporated into the matrix during the polymerisation.[115,116]

The modified IONPs can serve as either crosslinkers or templates around which the nanogel can be synthesised.

Gao *et al.* utilised the hydroxyl groups on the surface of bare IONPs to modify the surface with 2-isocyanatoethyl methacrylate (IEM).[108] The resulting IEM-IONPs were employed as templates for synthesising a PVCL nanogel with miniemulsion polymerisation. However, the hydrophobic nature of the IEM-modified IONPs caused aggregation in solution (with an average particle size of 215 nm in dimethylsulfoxide, while transmission electron microscopy (TEM) analysis indicated a diameter of 18 nm); the aggregation led to the presence of multiple particles within the core of the nanogel.

Similarly, Chen *et al.* employed 3-(trimethoxysilyl)propyl methacrylate (TMSPMA) as a ligand, which promoted IONPs aggregation.[117] These aggregated IONPs were used as crosslinking nodes in a PNIPAAM nanogel, but the resulting magnetic nanogel exhibited non-homogeneous crosslinking density. This unevenness can be attributed partially to the challenge of uniformly modifying IONPs with crosslinkers, resulting in different numbers of crosslinking sites per particle. Furthermore, the hydrophobic nature of TMSPMA contributed to the formation of clusters with varying dimensions, leading to differences in the number of crosslinking sites between the cores.

In 2021, Chou *et al.* obtained well-dispersed IONPs by imparting a negative charge on the surface. This was accomplished by using acrylic acid (AA) monomers as the surface active ligands.[118] The study emphasised the critical nature of anchoring AA, highlighting its importance in synthesising magnetic hydrogels with small encapsulated cores of IONPs. When no anchoring step was performed and all the components were blended, minimal incorporation of IONPs in the hydrogel matrix was observed.[118]

In a study by Fernandez *et al.* in 2021, the efficacy of the *grafting through* method was compared with that of the *blending* method. Using 3-butenoic acid as the surface-active monomer, the *blending* method resulted in IONPs predominantly located towards the surface of a continuous macrogel matrix.[119] In contrast, the *grafting through* method led to uniform localisation of IONPs at the centre of individual nanogels ranging between 100 and 200 nm in size.

The works by Fernandez *et al.* and Chou *et al.* demonstrate the superiority of the *grafting* methods over the methods utilising physical entrapment. *Grafting* methods offer superior control over both size and morphology, facilitating the core placement of the majority IONPs within the nanogel structure. However, the *grafting to* method can lead to a less dense coating due to the steric effects of bulky polymer chains.[109] Grafting a monomer onto IONP surfaces ensures uniform templating of the nanogel, although monomer solubility affects morphology, with poorly dispersed monomer-IONPs resulting in undesired clustering.[108,109,117] Nonetheless, the *grafting through* maintains composite size within the nanometer scale.[119] In some instances, it is possible to achieve a single core–shell configuration below 50 nm.[120] Thus, employing surface-active IONPs as templates in the *grafting through* method is preferred.

6. Properties

In the design of magnetic nanogels, a key concern lies in the impact of hybridisation on the properties of the individual components.[91] Coating or trapping the IONPs in the matrix will reduce their rotation, which influences the SAR. On the other hand, the volume phase transition of the nanogel can be impacted as a portion of the internal volume of the nanogel is occupied by the IONPs.[91] This interplay between the nanogel matrix and the encapsulated IONPs underscores the importance of understanding and optimising the hybridisation process to achieve desired properties in magnetic nanogels.

6.1 Magnetic properties

As mentioned, achieving effective hyperthermia treatment requires magnetic nanogels with high heating ability. However, the encapsulation of IONPs hinders their rotational movement, thereby reducing their Brownian relaxation and leading to a decrease in M_S and SAR, Table 2.

Medeiros *et al.* reported that magnetic hydrogels with the lowest percentage of iron content (0.08 wt%) exhibited the lowest M_S per mass unit of sample.[122] However, having a high concentration of IONPs in the core can adversely affect the thermo-responsiveness of the polymer.

Zhang and co-workers synthesised magnetic nanogels by polymerising PNIPAAM and chitosan in the presence of oleic

Table 2 Examples of magnetic hybrid systems and their MS, with and without polymer coatings. MEO2MA – (2-(2-methoxyethoxy)ethyl methacrylate); TMSPMA – 3-(trimethoxysilyl)propyl methacrylate

Components	M_S of composite (emu g^{-1})	M_S of bare IONPs (emu g^{-1})	Ref.
Fe$_3$O$_4$-MEO$_2$MA	14	51	119
PNIPAAM-(AA-Fe$_3$O$_4$)	1	63	118
PNIPAAM-TMSPMA-Fe$_3$O$_4$	9	60	117
Fe$_3$O$_4$-maleic anhydride	32	82	121
Fe$_3$O$_4$-chitosan-*g*-PVCL	37	57	95

acid-coated IONPs with the *blending* method.[123] The magnetic nanogel exhibited a M_S value of 9.3 emu g^{-1} sample, significantly lower than the 64.3 emu g^{-1} of the bare IONPs. As the oleic acid-coated IONPs also showed a decrease in M_S (35.8 emu g^{-1} sample), they concluded that:

• The oleic acid shell around the nanoparticles reduced the magnetic properties of the sample;

• The presence of a thick carbon shell in the magnetic nanogels reduced the magnetism of the particles by disrupting the surface anisotropy and the alignment of the surface spins.[123]

However, when subjected to an AMF, an increase in solution temperature was observed, dependent on the concentration of magnetic nanogels (10 g mL^{-1} 15–35 °C and 20 mg mL^{-1} 15–45 °C). Zhang and co-workers measure a SAR value between 10 and 15 W g^{-1} when exposing the magnetic nanogels to an AMF with an amplitude of 20 kA m^{-1} and a frequency of 360 kHz. This demonstrates that magnetic nanogels do not necessarily require high M_S to release heat to the environment; however, the SAR value is too low for hyperthermic applications.[123] Similarly, in the study by Chiu and co-workers, the M_S of the sample containing the IONPs synthesised with *blending* method decreased from 77 emu g^{-1} to 36 emu g^{-1} post-polymerisation.[106]

In the study by Gao *et al.*, minimal differences were observed in the M_S of the bare IONPs, the ligand-modified IONPs and the magnetic nanogel synthesised with the *grafting through* method (68 emu g^{-1}, 64 emu g^{-1} and 60 emu g^{-1} respectively).[108] However, no experiments to record the SAR value were performed. Similarly, the coating did not significantly impact the M_S values of the magnetic nanogels synthesised by Lin and co-worker.[124]

Recently, Cazares-Cortes *et al.* reported that the incorporation of 37.5 wt% IONPs in their nanogel through *grafting to* method did not affect the M_S (98 and 96 emu g^{-1}). Under an AMF with a frequency of 335 kHz and an amplitude of 7 kA m^{-1}, they recorded a SAR value of 47 W g^{-1}, comparable to that of the IONPs alone (SAR of 55 W g^{-1}). Their findings indicate that the right polymer formulation will not affect the magnetic properties of the IONPs,[113] but the SAR is lower than the ideal one for biomedical applications.[27] Other studies in the literature have also reported no reduction in the M_S of the magnetic core.[102,125] To illustrate the potential of their MagNanogel for hyperthermia therapy, Cazares-Cortes *et al.* demonstrated an increase of the water temperature from 20 °C to 40 °C in a solution of MagNanogels exposed to AMF.[113] Under AMF for 30 min, they observed a size change from 462 nm to 430 nm. This study showcased how IONPs can induce thermo-responsive behaviour in the surrounding polymer matrix.[113]

6.2 Thermo-responsiveness

When IONPs are encapsulated in the nanogel matrix, they could hinder the coil-to-globule transition and impact the LCST value of the composite.

For instance, Fernandez *et al.* utilised MEO$_2$MA as the thermosensitive polymer (LCST = 26 °C), but observed a transition temperature of 21.9 °C in the magnetic microgels.

The change in LCST is dependent on the synthesis of the magnetic nanogel and the chosen polymer. Chen *et al.* found that PNIPAAM magnetic microgels exhibited a transition temperature of around 33 °C, similar to that of PNIPAAM microgels (32 °C).[117]

Additionally, the percentage of iron content can affect the size change at the LCST.[122] Chou *et al.* recorded the transition temperature for magnetic nanogels with a P(PNIPAAM-*co*-AA) polymer blend synthesised with the *grafting through* method. The magnetic nanogels with a higher percentage of IONPs in the core exhibited less shrinkage.[118]

In another study by Gao *et al.*, magnetic nanogels synthesised with *grafting through* method with PVCL showed a clear size reduction (440 nm to 380 nm) in the temperature range between 28 °C to 42 °C, with an LCST of 32.5 °C.[108] No change was observed before or after this range. However, for a more precise therapy, the temperature range should be narrow to allow for a sharp decrease in size. Liu *et al.* achieved a narrow temperature range for their PVCL-based magnetic nanogel with the *grafting through* method, which shrank from 530 to 300 nm within approximately a 4 °C range, with an LCST of 40 °C.[125]

The environment can also influence the LCST of the polymer. Jiang *et al.* calculated an LCST of 40 °C for their magnetic nanogel with PNIPAAM.[126] However, by adjusting the pH of the medium, they were able to modify the LCST: at pH 6.8, the LCST was 37 °C due to the reduced hydrophilicity of the less ionised carboxyl groups of the PNIPAAM.

For hyperthermia applications, the nanogel should respond to temperatures above the body's and be stable in an acidic environment to prevent premature drug release.[125]

6.3 Drug release

Chemotherapy drugs can be loaded into magnetic nanogels and held in the matrix through various non-covalent interactions, such as hydrogen bonding[108] and electrostatic interactions,[127] or covalent conjugation.[126]

Liu *et al.* applied an external AMF to induce the release in their magnetic nanogels. The release of cargo only slightly increased with AMF.[125] Investigations revealed that the drug release was primarily driven by the dissociation of the nanogel shell in the presence of glucose. Consequently, the group concluded that AMF-triggered release made only a small contribution to the overall drug release mechanism.

Similarly, Gao *et al.* observed an increase in the percentage of drugs released by their magnetic nanogels when the solution temperature was increased to 37 °C. However, no tests were performed in the presence of an AMF. This suggests that drug release from this composite could occur simply by injecting it into the body due to the wide temperature range triggering release.[108]

Cazares-Cortes *et al.* were able to load up to 63% of doxorubicin (DOX) in their MagNanogel and tested the release

under heat, pH and magnetic trigger. By raising the temperature of a water bath to 50 °C and 70 °C, they could achieve up to 32 and 36% of release after 4 h.[113] Under AMF with amplitude 12 kA m^{-1} and frequency 335 Hz, the group achieved up to 47% DOX release. It is worth noting that close to 100% release was obtained when the pH was lowered from 7.5 to 5 as the MagNanogels are sensitive to the acidic environment.

The characteristics of magnetic nanogels are dependent upon both the size of IONPs and the polymer utilised. However, magnetic nanogels synthesised *via* the *grafting through* technique preserve the inherent properties of their constituent elements. This phenomenon stems from the enhanced control achieved through covalent synthetic methods for incorporating IONPs, contrasting with the limitations of physical entrapment approaches. However, very few studies in the literature present a complete set of data, in particular regarding the response to the AMF and measurement of the SAR value. Among the reported magnetic nanogels, the work by Cazares-Cortes *et al.* appears to be the most promising for drug release and thermo-responsiveness. Despite preserving the magnetic properties of the IONPs post-nanogel synthesis and promising experiments in solution, the relatively low SAR value (47 W g^{-1}) might hinder biomedical applications *in vivo*.

7 Applicability of magnetic nanogels for cancer treatment

7.1 Biocompatibility of magnetic nanogels

Several studies have reported the good biocompatibility of magnetic nanogels,[95] which seem to be less cytotoxic to healthy cells than certain chemotherapy drugs, such as DOX,[113,124] while exhibiting higher efficiency against cancer cells.[113,127]

7.1.1 *In vitro* studies. Indulekha *et al.* investigated the cytotoxicity of 1 mg mL^{-1} of magnetic nanogel containing 0.42 mg mL^{-1} of DOX in breast cancer cells.[95] At room temperature, the viability of the cells treated with the magnetic nano gels-DOX was 60%, whereas cells treated with 0.42 mg mL^{-1} of DOX alone exhibited a viability of 40%.[95]

The magnetic nanogel developed by Cazares-Cortes *et al.* showed viability close to 100% for cells treated with 2 mM of the composites, while cells treated with DOX alone showed viability of only 60%.[113]

Magnetic polymers containing poly(acrylic acid), such as those synthesised by Sundaresan *et al.*, also exhibited good biocompatibility (80% viability with 0.5 mg mL^{-1}), challenging the toxicity associated with the acrylate units.[128] The magnetic nanogel developed by Mdlovu *et al.* contains pluronic F127 (PF) and polyethylenimine (PEI). PEI is known for its cell toxicity.[124] No cell death was observed in HepG2 cells after 24 h and 48 h with concentrations of up to 75 μL mL^{-1} of the magnetic nanogel.

Once DOX was loaded in the magnetic nanogel and tested against cancer cells, the complex was found to be less cytotoxic than the drug alone.[124] However, when the cells were exposed to an external magnetic field, the viability was lower than that observed with DOX alone. The team was able to verify an increased presence of DOX inside the cells when delivered with the magnetic nanogel. This suggests that the PF/PEI nanogel can destabilise the endosomal barriers and facilitate penetration of DOX through the cellular membrane.

7.1.2 *In vivo* studies. Zhang *et al.* conducted *in vivo* studies to assess the toxicity of a magnetic nanogel containing PNIPAAM and AA monomers. Mice treated with DOX alone exhibited severe degradation of the liver, whereas no damage was observed in those treated with the magnetic nanogel.[129]

Jiang *et al.* found no iron accumulation in the animals' organs after 21 d from the treatment with the magnetic nanogel. Histopathological exams on the liver, spleen, brain, and other organs did not show any abnormal results.[126]

7.2 Efficiency of the combined hyperthermia/drug delivery system

Despite the abundance of literature on the synthesis and properties of magnetic nanogels, few studies have extended their investigations to include *in vitro* experiments. To the authors' knowledge, no paper has explored the *in vivo* efficacy of magnetic nanogels for combined hyperthermia and drug delivery. Therefore, in the *in vivo* section, the two cited works should be considered exemplary studies outlining the necessary experiments for a comprehensive investigation.

7.2.1 *In vitro* studies. Sundarsen *et al.* compared the cell death induced by DOX and by the DOX-magnetic nanogel after incubation at 37 °C and 40 °C. As expected, at 40 °C, viability was 54% for DOX and 42% for the magnetic system. At 37 °C, 26% of the cells were killed by DOX and 19% by the magnetic system. These results indicated that, below the LCST, the drug within the polymer is not able to diffuse through the pores.[128]

Cazares-Cortes *et al.* compared the viability of cancer cells with and without the contribution of the AMF. Empty magnetic nanogels under AMF did not affect the cells' viability. After loading DOX in the magnetic nanogel, 75% of the cells died after exposure to AMF (with a local temperature of 65 °C). As 50% died without AMF, the paper concluded that hyperthermia enhances the cytotoxicity of DOX but is not efficient on its own.[113]

Contrary to Cazares-Cortes *et al.*,[113] Indulekha *et al.* reported that 2 mg mL^{-1} of the empty magnetic nanogels under AMF caused 51% of cell death.[95] After DOX loading, the magnetic nanogels were found to be toxic to 50% of the cells without AMF and to 80% with AMF. It should be noted that the DOX-loaded magnetic nanogels in a water bath at 43 °C released 60% of DOX under AMF and 40% without. Hence, the highest cytotoxicity of the DOX-loaded magnetic nanogels under AMF could be attributed to a higher amount of DOX released in the cells rather than due to the hyperthermic action.[95]

7.2.2 *In vivo* studies. Zhang *et al.* demonstrated the enhanced efficacy of DOX when encapsulated in a magnetic nanogel using a mouse model. However, in this magnetic

nanogel, the pH was used as the trigger for drug release and no hyperthermia work was done. The group found a significant reduction in liver tumour size upon treatment with targeted and DOX-loaded magnetic nanogels after 14 d. While the saline group tumour was 473 mm^3, the volumes of the tumours treated with the magnetic nanogels were found to be 135 and 109 mm^3. For comparison, the volume of the tumour treated with DOX alone was around 300 mm^3. This reduction in tumour volume is attributed to the controlled and sustained release of the encapsulated drug over time, highlighting the potential of magnetic nanogels as drug delivery systems for cancer therapy.[129] As the body weight of the mice treated with magnetic nanogels remained constant throughout the administration window, the group concluded that the magnetic nanogels did not have a toxic effect on the organism.

A study conducted by Hayashi et al. demonstrates the synergistic effect of combined therapy in a mouse model with xenografted tumours. In their experiment, IONPs coated with polymer chains were injected into the mice, followed by the application of an AMF.[130]

Thermal imaging of the animals revealed the localised "hot-spot" effect generated by the IONPs when exposed to the AMF, Fig. 13. Subsequent monitoring of tumour reduction over several days post-treatment showed a significant decrease in tumour size.

Fig. 14 depicts the mice 45 d after the injection, illustrating an 80% reduction in tumour size in mice treated with either hyperthermia or chemotherapy alone. Notably, in mice treated with the magnetic composite under AMF, the tumour completely disappeared after 12 d. Furthermore, the survival rate of

the mice treated with the combined chemotherapy and hyperthermia was 100% after 200 d from the treatment. Mice treated with the individual treatments died after 100 d from the procedure.[130]

This data suggests a synergistic mechanism wherein magnetic hyperthermia treatment reduces the volume of tumour cells, facilitating the penetration and efficacy of chemotherapy drugs throughout the tumour tissue.[130]

To conclude, several formulations in the literature have demonstrated the non-toxicity of magnetic nanogels. However, there is a lack of in vitro and in vivo studies showing the efficacy of magnetic nanogels for combined hyperthermia and chemotherapy. The in vitro works done by Indulekha et al.[131] and by Cazares-Cortes et al.[113] have both shown that around 75 to 80% of cancer cells can be killed with DOX-loaded magnetic nanogels under AMF. As the SAR of the MagNanogels by Cazares-Cortes et al. might not be ideal for human applications, there is an urgent need for in vivo studies.

8. Beyond iron oxide magnetic nanogels

In recent years, the field of magnetic nanogels has witnessed significant advancements, with the integration of various materials to enhance their properties and broaden their applications, Fig. 15.

8.1 Magnetic graphene oxide nanogels

The incorporation of graphene oxide (GO) into magnetic nanogels offers several advantages,[132] including increased drug-loading capacity and the ability for magnetic tracking and smart drug delivery.[133]

Bardajee et al. demonstrated a method for modifying GO with magnetic nanoparticles to create magnetic GO (MGO). While the MGO nanogels showed high drug loading efficiency (more than 80% for DOX), the relatively low M_S of 0.08 emu g^{-1} limited their suitability for applications such as hyperthermia, MRI, or magnetic guiding.[132]

In contrast, Kunene et al. achieved higher M_S and superparamagnetic behaviour for both MGO and MGO nanogels (71.62 and 67.61 emu g^{-1}, respectively).[134]

Despite the reduction in porosity due to the presence of nanogels, they demonstrated higher loading efficiency of MGO nanogels compared to MGO alone. Moreover, they observed accelerated drug release from MGO nanogels under the influence of an AMF, high temperatures, and acidic pH conditions.[134]

8.2 Magnetic-fluorescent nanogels

The integration of quantum dots (QDs) into magnetic nanogel formulations offers the potential to impart fluorescence to the structure, enabling sensing capabilities[135] and cellular imaging.[136]

Shen et al. synthesised a luminescent-magnetic nanogel by incorporating pre-formed IONPs and QD during the polymeris-

Fig. 13 Thermal image of a mouse injected with magnetic polymer grafts.[130] Adapted with permission from M. Hayashi et al., *Theranostics*, 2014, **4**, 834–84. Copyright 2014 Ivyspring International Publisher.
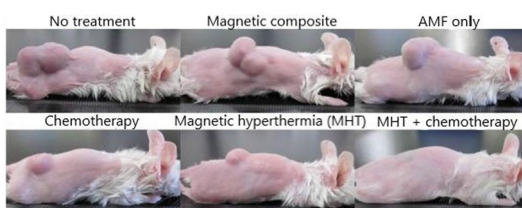
Fig. 14 Pictures of tumour size after 45 d of treatment.[130] Adapted with permission from M. Hayashi et al., *Theranostics*, 2014, **4**, 834–84. Copyright 2014 Ivyspring International Publisher.
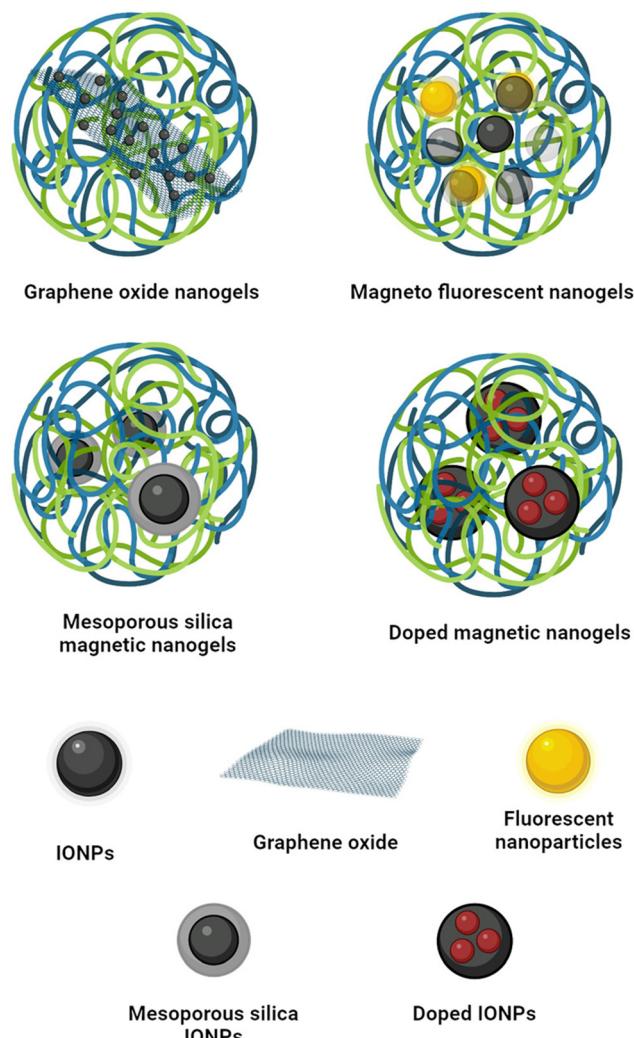
Fig. 15 Other magnetic nanogel structures found in the literature (created with Biorender.com).

ation of chitosan.[136] The composite showed strong orange/yellow emission, making it suitable for imaging purposes. However, the presence of cadmium in the QDs had a slight impact on cell viability due to its toxicity.[136]

In a different approach, Wang *et al.* developed a core–shell nanogel containing iron oxide crystals and non-toxic[137] fluorescent carbon dots (CDs).[138] Similar to magnetic nanogels, these composite nanogels were capable of releasing heat induced by the IONPs under an AMF. Additionally, the CDs enabled the nanogels to absorb near-infrared (NIR) wavelengths, allowing them to heat the environment upon NIR irradiation.[138] Consequently, these nanogels could be utilised for both hyperthermia and photothermal therapy, with triggering mechanisms involving either an external AMF or NIR irradiation. Furthermore, the magnetic-fluorescent nanogels could be employed for fluorescent tracking, as the luminescence intensity was dependent on the size, with emission intensity increasing as the matrix shrank.[138]

8.3 Mesoporous silica magnetic nanogels

Coating the IONPs with a mesoporous silica shell (MSS) is one of the most widely used strategies to improve the biocompatibility of the IONPs and increase the particles' surface area for improved drug loading abilities.[139] While silica itself does not release drugs on cue, incorporating a nanogel coating can enable smart release mechanisms.[140]

Mdlovu *et al.* demonstrated that incorporating stimuli-responsive nanogels enhances the loading efficiency of IONPs coated in mesoporous silica.[124] Their magnetic nanogel showed a sustained release for over 70 h, with the highest release (94.41%) reached at an acidic pH of 5.4 and 42 °C due to the thermoresponsivity of the nanogel. Although these conditions mimic the altered physiology of the tumour environment, release experiments in the presence of an AMF were not conducted. *In vitro* and *in vivo* experiments showed no toxicity during histopathological analyses and enhanced tumour reduction in mice.[124]

The presence of silica on the surface of IONPs can significantly reduce their magnetism.[140,141] Despite this, the MSS-IONPs nanogel reported by Keshavarz *et al.* exhibited a SAR value of 108.6 W g^{-1} and a temperature of 58 °C within 5 min of exposure to an AMF.[140] The frequency and intensity of the magnetic field were 315 kHz and 14.3 kA m^{-1} respectively. The application of an AMF increased cargo release from 15% to 70%, demonstrating potential applications in hyperthermia and triggered drug release.

8.4 Doped mangnetic nanogels

Doping IONPs with other elements, such as manganese or zinc, can enhance their magnetic properties, stability, and SAR, making them more suitable for biomedical applications.[142]

Monfared *et al.* utilised manganese zinc ferrite nanoparticles as the magnetic component in their PNIPAAM nanogel formulation.[143] The resulting nanogel exhibited a SAR of 62.4 W g^{-1} in an AMF with 10 kA m^{-1} amplitude and 400 kHz frequency. The nanogel showed the highest sustained release of the drug when incubated at 44 °C for 24 h. However, it's important to note that no experiments were conducted to investigate drug release induced by an AMF. This aspect is crucial for evaluating the feasibility of using such nanogels in magnetic field-triggered drug delivery systems. Further studies are needed to explore the responsiveness of these doped IONP-based nanogels to external magnetic stimuli and their potential for controlled drug release in hyperthermia applications.

9. Challenges for clinical applications

The translation of research findings from the laboratory to clinical trials faces numerous challenges, resulting in a limited number of studies advancing to clinical stages.[4] Several reasons contribute to this gap between research and clinical application, as outlined in various reviews[144–146] and have been summarised in this section. The lack of international

standards for assessing the safety of nanomedicines poses a significant obstacle to their commercialisation.[146] Existing toxicological guidelines within both the European and American Pharmacopeias address general safety assessments, but they are not specific to nanomaterials. Nanoparticles exhibit unique behaviours due to their size, necessitating specialised regulations for their production and physico-chemical testing.[144,145] Furthermore, guidelines for studying the pharmacokinetics profiles of nanomaterials are lacking in regulatory agencies such as the Food and Drug Administration (FDA), the Medicines and Healthcare products Regulatory Agency (MHRA) and the European Medicines Agency (EMA). Nanomaterials' pharmacokinetics and pharmacodynamics profiles are more complex than traditional drugs, involving factors like protein corona formation, intricate metabolic pathways, and potential body accumulation.[147]

Understanding how nanomaterials behave in the biological environment is crucial before their commercialisation.[146] While *in vitro* and small animal studies provide valuable insights, the human biological environment differs significantly, making it challenging to predict nanomedicine behaviour post-administration.[4] Despite the extensive research on nanomaterials, there is a significant gap in toxicological studies specific to nanomaterials.[147] Developing new nanotoxicological assays, such as microfluidics or organ bioprinting, is essential for translating nanomedicines into clinical applications.[147]

Furthermore, the absence of specific regulations on good manufacturing practices, laboratory practices, and clinical practices for nanomaterials poses a challenge.[147] International regulations could help prevent instances such as the removal of approved nanotechnological formulations from the market due to unforeseen negative side effects.[144]

The transition from laboratory-scale development to industrial-scale production presents a significant obstacle in the commercialisation of nanomaterials and nanomedicine. Firstly, nanoparticle production is exceptionally sensitive to minute variations.[148] Factors like stirring speed and agitation, crucial in maintaining formulation integrity, can exert substantial influence.[149] Scaling up to larger batches highlights the issue and ensuring reproducibility becomes increasingly difficult. Any inconsistency in batch-to-batch uniformity could result in altered properties and physicochemical profiles of the drug.[148] However, the multitude of parameters necessary to ensure product uniformity renders purity validation challenging. Moreover, the synthetic pathways of nanomedicines often involve multi-step, complex processes that are low-yielding and high-cost, dissuading pharmaceutical manufacturing efforts.[148] The presence of solvents and potentially toxic components such as unreacted monomers or ligands complicates purification procedures, without guaranteeing product purity and safety.[148] Finally, verifying the stability of nanomedicine throughout production, storage, and administration is paramount, as even slight alterations could impact drug toxicity.[148] These various challenges collectively contribute to the complexity of establishing the requisite quality control assess-ments necessary for the commercialisation of nanomedicines.[149]

Despite FDA approval or clinical trials for both IONPs[145] and nanogels,[144] no magnetic nanogel has entered human trials. While NanoTherm® (IONPs coated in aminosilane) has been successfully commercialised,[10] ThermoDox® (a liposome formulation) reached phase III clinical trial before being halted due to insufficient evidence of efficacy.[150] Despite this setback, the success of NanoTherm® paves the way for magnetic nanogel formulations as efficient synergistic therapies against cancer.

Finally, the intrinsic limitations of the magnetic field applicable in hyperthermia therapy pose a challenge to the development of magnetic nanogels.[151] The heat generated during hyperthermia therapy is partly due to eddy currents, which are induced by metallic materials in magnetic fields and are quantified by the following equation:

$$P = \sigma_t (\pi \mu_0)^2 (H_0 f)^2 r^2$$

where P is the power density, σ_t is the electrical conductivity of the tissue, μ_0 is the vacuum permeability, H_0 is the amplitude of a magnetic field, f is the frequency and r is the radius of the object conveying the hyperthermia.[152] It is important to note that the intensity of the eddy current is proportional to the square of the r. Consequently, beyond a certain product value of H_0 and f ($H_0 \times f$), there is a risk of heating healthy tissue distant from the tumour site. This critical value is known as the Atkinson–Brezovich limit, established at 4.85×10^8 Am s^{-1}.[152] In 2004, this limit has been increased to 1.8×10^9 Am s^{-1}, as demonstrated by NanoTherm®'s magnetic field parameters (18 kA m^{-1} and 100 kHz)[153] which were found to be safe for patients. Since 2006, several *in vivo* experiments have suggested that this limit can be further increased.[154–157] Caizer reported an optimal value of 5×10^9 Am s^{-1} for particles with a diameter within 16 to 17 nm, with H_0 between 10–25 kA m^{-1} and f between 200–500 kHz (as long as $H_0 \times f$ is respected).[158] Herrero de la Parte *et al.* proposed a new limit of 9.46×10^9 Am s^{-1}, achieved with a frequency of 591 kHz and an amplitude of 14 kA m^{-1}.[159] However, higher values have been observed to be harmful to healthy rodents. It should also be considered that patients who are already weakened due to surgery or the presence of a tumour might not tolerate such high levels of magnetic field intensity and amplitude.[159] Overall, there is a lack of studies concerning the safe limits of magnetic fields during hyperthermia therapy.[38] In 2023, Kwok *et al.* argued that the Atkinson–Brezovich limit is prone to misuse and may not be the best metric for safety.[160] Hence, the authors proposed a new metric, the SAR$_{MAX}$, as a parameter to determine acceptable levels of magnetic hyperthermia. SAR$_{MAX}$ describes the maximum power absorbed per unit mass of tissue due to eddy currents, averaged over 10 g of tissue and 6 min. As a guideline, should not exceed 20 mW g^{-1} for the torso or head (achieved with f of 330 kHz and H of 4.9 kA m^{-1}) and 40 mW g^{-1} for the limbs (f of 242 kHz and

maximum H of 10.43 kA m^{-1}).[160] The paper identifies several advantages for this new parameter, namely:

• The possibility of establishing a correlation with the local SAR limits for MRI.

• SAR$_{MAX}$ can be easily estimated from calculations, simulations, or direct measurements.

• This parameter is reliable and adaptable, accounting for hot spots and non-axial field geometries.

In the study by Kwok et al., the patients did not experience any discomfort during the hyperthermia experiments.[160]

Overcoming these challenges requires interdisciplinary collaborations, innovative approaches, and sustained investment in translational research. Despite hurdles, ongoing efforts aim to advance the clinical translation of nanomaterial-based therapies, ultimately improving patient outcomes and advancing healthcare.

10. Conclusions

Combining hyperthermia and chemotherapy through magnetic nanogels presents a promising approach in cancer treatment, offering synergistic therapeutic effects and addressing the limitations of individual treatments.[3,4]

While various synthesis strategies exist for magnetic nanogels, optimising their magnetic properties, thermo-responsiveness, drug-loading capacity, and biocompatibility are crucial for their effectiveness.[76] Optimisation of the magnetic properties and SAR for hyperthermic properties is still needed to achieve the optimal value for biomedical applications. Numerous studies in this review have thoroughly investigated the thermo-responsive characteristics of magnetic nanogels, additional research focusing on drug release upon exposure to AMF is needed.

Although there is ongoing debate regarding the cytotoxicity of hyperthermia alone, studies have demonstrated the efficacy of magnetic nanogels in combined hyperthermia and chemotherapy drug delivery in vitro. However, challenges such as the complexity of magnetic nanogels, limited understanding of their behaviour in vivo, and their multi-component nature hinder their translation into clinical applications.[146] Conducting in vivo comparisons to assess the potential increased toxicity of magnetic nanogels compared to individual hyperthermia and chemotherapy treatments would advance the field towards commercialisation. Data on the tumour regression, toxicity and survival rate of mice treated with magnetic nanogels could bridge the gap between the bench and the market. Similarly, a comparative study against other formulations for combined hyperthermia and chemotherapy, such as magnetic liposomes, would demonstrate the advantages of nanogels over other combined therapy approaches.

Most studies in the literature utilise spherical IONPs in magnetic nanogels, but exploring alternative morphologies such as cubes and nanoflowers could offer enhanced heating abilities and therapeutic efficacy. Further research into the pro-

perties and behaviour of magnetic nanogels, along with the development of standardised protocols, will be crucial for advancing their clinical translation and realising their potential in cancer therapy.[107]

Author contributions

Sofia Patri: Conceptualisation (supporting); writing – original draft (lead); writing – review and editing (equal). Nguyen T. K. Thanh: Conceptualisation (lead); writing – review and editing (equal). Nazila Kamaly: Conceptualisation (lead); writing – review and editing (equal).

Data availability

As this is a review article, the Data availability statement does not apply.

Conflicts of interest

There are no conflicts to declare.

Acknowledgements

References

1 Y. Sun and E. Davis, Nanomaterials, 2021, 11, 746.

2 D. Longley and P. Johnston, J. Pathol., 2005, 205, 275–292.

3 K. Bhatia, Bhumika and A. Das, Life Sci., 2020, 258, 118134.

4 M. J. Mitchell, M. M. Billingsley, R. M. Haley, M. E. Wechsler, N. A. Peppas and R. Langer, Nat. Rev. Drug Discovery, 2021, 20, 101–124.

5 R. D. Issels, L. H. Lindner, J. Verweij, R. Wessalowski, P. Reichardt, P. Wust, P. Ghadjar, P. Hohenberger, M. Angele, C. Salat, Z. Vujaskovic, S. Daugaard, O. Mella, U. Mansmann, H. R. D. T. Knösel, S. Abdel-Rahman, M. Schmidt, W. Hiddemann, K.-W. Jauch, C. Belka and A. Gronchi, JAMA Oncol., 2018, 4, 483–492.

6 Z. Behrouzkia, Z. Joveini, B. Keshavarzi, N. Eyvazzadeh and R. Aghdam, Oman Med. J., 2016, 31, 89–90.

7 B. Hildebrandt, P. Wust, O. Ahlers, A. Dieing, G. Sreenivasa, T. Kerner, R. Felix and H. Riess, Crit. Rev. Oncol., 2002, 43, 33–56.

8 B. Woodhall, K. Pickrell, N. Georgiade, M. Mahaley and H. Dukes, Ann. Surg., 1960, 151, 750–758.

9 P. Wust, B. Hildebrandt, G. Sreenivasa, B. Rau, J. Gellermann, H. Riess, R. Felix and P. Schlag, *Lancet Oncol.*, 2002, **3**, 487–497.

10 F. Soetaert, P. Korangath, D. Serantes, S. Fiering and R. Ivkov, *Recent Adv. Drug Delivery Res.*, 2020, **163**, 65–83.

11 E. Guisasola, A. Baeza, L. Asín, J. M. dela Fuente and M. Vallet-Regí, *Small Methods*, 2018, **2**, 1800007–1800018.

12 D. Ortega, in *Magnetic Nanoparticles: From Fabrication to Clinical Applications: Structure and Magnetism in Magnetic Nanoparticles*, ed. N. T. K. Thanh, CRC Press, Taylor & Francis group, 1st edn, 2012.

13 N. Hoshyar, S. Gray, H. Han and G. Bao, *Nanomedicine*, 2016, **11**, 673–692.

14 A. K. Gupta and M. Gupta, *Biomaterials*, 2005, **26**, 3995–4021.

15 N. Feltin and M. P. Pileni, *Langmuir*, 1997, **13**, 3927–3933.

16 P. Majewski and B. Thierry, *Crit. Rev. Solid State Mater. Sci.*, 2007, **32**, 203–215.

17 L. Asín, G. Stepien, M. Moros, R. M. Fratila and J. M. de la Fuente, in *Clinical Applications of magnetic nanoparticles, Magnetic Nanoparticles for Cancer Treatment Using Magnetic Hyperthermia*, ed. N. T. K. Thanh, CRC Press, Taylor & Francis group, 1st edn, 2019.

18 L. Lartigue, P. Hugounenq, D. Alloyeau, S. P. Clarke, M. Lévy, J.-C. Bacri, R. Bazzi, D. F. Brougham, C. Wilhelm and F. Gazeau, *ACS Nano*, 2012, **6**, 10935–10949.

19 B. S. Kwon, W. Zhang, Z. Li and K. M. Krishnan, *Adv. Mater. Interfaces*, 2015, **2**, 1400511.

20 P. Atkins, J. D. Paula and J. Keeler, in *Atkins' Physical chemistry*, Oxford University Press, Oxford, 11th edn, 2018, ch. 15, p. 675.

21 A. Hervault and N. T. K. Thanh, *Nanoscale*, 2014, **6**, 11553–11573.

22 Q. Li, C. W. Kartikowati, S. Horie, T. Ogi, T. Iwaki and K. Okuyama, *Sci. Rep.*, 2017, **7**, 9894.

23 A. P. LaGrow, M. O. Besenhard, A. Hodzic, A. Sergides, L. K. Bogart, A. Gavriilidis and N. T. K. Thanh, *Nanoscale*, 2019, **11**, 6620–6628.

24 N. A. Stocke, P. Sethi, A. Jyoti, R. Chan, S. M. Arnold, J. Z. Hilt and M. Upreti, *Biomaterials*, 2017, **120**, 115–125.

25 U. Gneveckow, A. Jordan, R. Scholz, V. Brüß, N. Waldöfner, J. Ricke, A. Feussner, B. Hildebrandt, B. Rau and P. Wust, *Med. Phys.*, 2004, **31**, 1444–1451.

26 M. Johannsen, U. Gneveckow, L. Eckelt, A. Feussner, N. Waldöfner, R. Scholz, S. Deger, P. Wust, S. A. Loening and A. Jordan, *Int. J. Hyperthermia*, 2005, **21**, 637–647.

27 P. Wust, U. Gneveckow, M. Johannsen, D. Böhmer, T. Henkel, F. Kahmann, J. Sehouli, R. Felix, J. Ricke and A. Jordan, *Int. J. Hyperthermia*, 2006, **22**, 673–685.

28 M. Kallumadil, M. Tada, T. Nakagawa, M. Abe, P. Southern and Q. A. Pankhurst, *J. Magn. Magn. Mater.*, 2009, **321**, 1509–1513.

29 C. Martinez-Boubeta, K. Simeonidis, A. Makridis, M. Angelakeris, O. Iglesias, P. Guardia, A. Cabot, L. Yedra, S. E. F. Peiro, Z. Saghi, P. A. Midgley, I. C.-L. D. Serantes and D. Baldomir, *Sci. Rep.*, 2013, **3**, 1652–1659.

30 A. Meffre, B. Mehdaoui, V. Kelsen, P. F. Fazzini, J. Carrey, S. Lachaize, M. Respaud and B. Chaudret, *Nano Lett.*, 2012, **12**, 4722–4728.

31 R. D. Corato, A. Espinosa, L. Lartigue, M. Tharaud, S. Chat, T. Pellegrino, C. Ménager, F. Gazeau and C. Wilhelm, *Biomaterials*, 2014, **35**, 6400–6411.

32 E. Y. K. N. Suriyanto and S. D. Kumar, *Biomed. Eng. OnLine*, 2017, **16**, 1–22.

33 M. Suto, Y. Hirota, H. Mamiya, A. Fujita, R. Kasuya, K. Tohji and B. Jeyadevan, *J. Magn. Magn. Mater.*, 2009, **321**, 1493–1496.

34 X. Peng, B. Wang, Y. Yang, Y. Zhang, Y. Liu, Y. He, C. Zhang and H. Fan, *ACS Biomater. Sci. Eng.*, 2019, **5**, 1635–1644.

35 S. Mahjoob and K. Vafai, *Int. J. Heat Mass Transfer*, 2009, **52**, 1608–1618.

36 E. C. Abenojar, S. Wickramasinghe, J. Bas-Concepion and A. C. S. Samia, *Prog. Nat. Sci.: Mater. Int.*, 2016, **26**, 440–448.

37 S. Laurent, S. Dutz, U. O. Häfeli and M. Mahmoudi, *Adv. Colloid Interface Sci.*, 2011, **166**, 8–23.

38 D. Chang, M. Lim, J. A. C. M. Goos, R. Qiao, Y. Y. N. Y. Ng, F. M. Mansfeld, M. Jackson, T. P. Davis and M. Kavallaris, *Front. Pharmacol.*, 2018, **9**, 1–20.

39 S. Dutz and R. Hergt, *J. Am. Chem. Soc.*, 2014, **25**, 452001–452029.

40 K. M. Krishnan, *IEEE Trans. Magn.*, 2010, **46**, 2523–2558.

41 H. Arami, A. Khandhar, D. Liggitt and K. M. Krishnan, *Chem. Soc. Rev.*, 2015, **44**, 8576–8607.

42 U. Patil, S. Adireddy, A. Jaiswal, S. Mandava, B. Lee and D. Chrisey, *Int. J. Mol. Sci.*, 2015, **16**, 24417–24450.

43 Q. Feng, Y. Liu, J. Huang, K. Chen, J. Huang and K. Xiao, *Sci. Rep.*, 2018, **2**, 2082–2095.

44 T. K. Jain, M. K. Reddy, M. A. Morales, D. L. Leslie-Pelecky and V. Labhasetwar, *Mol. Pharmaceutics*, 2008, **5**, 316–327.

45 G. Liu, J. Gao, H. Ai and X. Chen, *Small*, 2013, **9**, 1533–1545.

46 M. Mahmoudi, H. Hofmann, B. Rothen-Rutishauser and A. Petri-Fink, *Chem. Rev.*, 2012, **112**, 2323–2338.

47 M. Lundqvist, J. Stigler, G. Elia, I. Lynch, T. Cedervall and K. A. Dawson, *Proc. Natl. Acad. Sci. U. S. A.*, 2008, **105**, 14265–14270.

48 N. Lewinski, V. Colvin and R. Drezek, *Small*, 2008, **4**, 26–49.

49 D. D. Stueber, J. Villanova, I. Aponte, Z. Xiao and V. L. Colvin, *Pharmaceutics*, 2021, **13**, 943–969.

50 L. Yildirimer, N. T. Thanh, M. Loizidoua and A. M. Seifalianh, *Nano Today*, 2011, **6**, 585–607.

51 A. Walter, A. Garofalo, A. Parat, H. Martinez, D. Felder-Flesch and S. Begin-Colin, *Nanotechnol. Rev.*, 2015, **4**, 581–593.

52 A. Walter, A. Garofalo, A. Parat, J. Jouhannaud, G. Pourroy, E. Voirin, S. Laurent, P. Bonazza, J. Taleb, C. Billotey, L. V. Elst, R. N. Muller, S. Begin-Colin and D. Felder-Flesch, *J. Mater. Chem. B*, 2015, **3**, 1484–1494.

53 Z.-T. Tsai, J.-F. Wang, H.-Y. Kuo, C.-R. Shen, J.-J. Wang and T.-C. Yen, *J. Magn. Magn. Mater.*, 2010, **322**, 208–213.

54 P. T. Yin, S. Shah, N. Pasquale, O. Garbuzenko, T. Minko and K. Lee, *Biomaterials*, 2016, **81**, 46–57.

55 C.-H. Fan, C.-Y. Ting, H.-J. Lin, C.-H. Wang, H.-L. Liu, T.-C. Yen and C.-K. Yeh, *Biomaterials*, 2013, **34**, 3706–3715.

56 A. Hervault, M. Lim, C. Boyer, A. Dunn, D. Mott, S. Maenosono and N. Thanh, *Nanoscale*, 2016, **8**, 12152–12161.

57 L. Wang, A. Hervault, P. Southern, O. Sandre, F. Couillaud and N. Thanh, *J. Mater. Chem. B*, 2020, **8**, 10527–10539.

58 K. Madaan, S. Kumar, N. Pooni, V. Lather and D. Pandita, *J. Pharm. BioAllied Sci.*, 2014, **6**, 139–150.

59 J. W. Bulte, T. Douglas, B. Witwer, S. C. Zhang, E. Strable, B. K. Lewis, H. Zywickea, B. Miller, P. van Gelderen, B. M. Moskowitz, I. D. Duncan and J. A. Frank, *Nat. Biotechnol.*, 2001, **19**, 1141–1147.

60 N. Hanafy, M. El-Kemary and S. Leporatti, *Cancers*, 2018, **10**, 238.

61 B.-S. Kim, J.-M. Qiu, J.-P. Wang and T. A. Taton, *Nano Lett.*, 2005, **5**, 1987–1991.

62 F. Yang, Y. Li, Z. Chen, Y. Zhang, J. Wu and N. Gu, *Biomaterials*, 2009, **30**, 3882–3890.

63 J. Xie, C. Xu, N. Kohler and S. S. Y. Hou, *Adv. Mater.*, 2007, **19**, 3163–3166.

64 J. L. Zhang, R. S. Srivastava and R. D. K. Misra, *Langmuir*, 2007, **23**, 6342–6351.

65 E. Strable, J. W. M. Bulte, B. Moskowitz, K. Vivekanandan, M. Allen and T. Douglas, *Chem. Mater.*, 2001, **13**, 2201–2209.

66 T. K. Jain, M. A. Morales, S. K. Sahoo, D. L. Leslie-Pelecky and V. Labhasetwar, *Mol. Pharm.*, 2005, **2**, 194–205.

67 Y. Chen, A. Bose and G. D. Bothun, *ACS Nano*, 2010, **4**, 3215–3221.

68 A. Hardiansyah, L.-Y. Huang, M.-C. Yang, T.-Y. Liu, S.-C. Tsai, C.-Y. Yang, C.-Y. Kuo, T.-Y. Chan, H.-M. Zou, W.-N. Lian and C.-H. Lin, *Nanoscale Res. Lett.*, 2014, **9**, 497.

69 Z. Al-Ahmady, N. Lozano, K.-C. Mei, W. T. Al-Jamal and K. Kostarelos, *Int. J. Pharm.*, 2016, **154**, 133–142.

70 H. Liu, C. Wang, Q. Gao, X. Liu and Z. Tong, *Acta Biomater.*, 2010, **6**, 275–281.

71 R. Narain, M. Gonzales, A. S. Hoffman, P. S. Stayton and K. M. Krishnan, *Langmuir*, 2007, **23**, 6299–6304.

72 S. A. Meenach, C. G. Otu, K. W. Anderson and J. Z. Hilt, *Int. J. Pharm.*, 2012, **427**, 177–184.

73 S. Dagdelen, M. Mackiewicz, M. Osial, E. Waleka-Bargiel, J. Romanski, P. Krysinski and M. Karbarz, *J. Mater. Sci.*, 2023, **58**, 4094–4114.

74 H. Ma, G. Yu, J. Cheng, L. Song, Z. Zhou, Y. Zhao, Q. Zhao, L. Liu, X. Wei and M. Yang, *Biomacromolecules*, 2023, **24**, 868–885.

75 R. T. Chacko, J. Ventura, J. Zhuang and S. Thayumanavan, *Adv. Drug Delivery Rev.*, 2012, **64**, 836–851.

76 A. A. Ali, A. Al-Othman and M. H. Al-Sayah, *J. Controlled. Release*, 2022, **351**, 476–503.

77 J. K. Oh, R. Drumright, D. J. Siegwart and K. Matyjaszewski, *Prog. Polym. Sci.*, 2008, **33**, 448–477.

78 E. Mauri, G. Perale and F. Rossi, *ACS Appl. Nano Mater.*, 2018, **1**, 6525–6541.

79 H. Wang, L. Gao, T. Fan, C. Zhang, B. Zhang, O. A. Al-Hartomy, A. Al-Ghamdi, S. Wageh, M. Qiu and H. Zhang, *ACS Appl. Mater. Interfaces*, 2021, **13**, 54621–54647.

80 J. K. Oh, D. J. Siegwart, H. Lee, G. Sherwood, L. Peteanu, J. O. Hollinger, K. Kataoka and K. Matyjaszewski, *J. Am. Chem. Soc.*, 2007, **129**, 5939–5945.

81 D. Steinhilber, M. Witting, X. Zhang, M. Staegemann, F. Paulus, W. Friess, S. Küchler and R. Haag, *J. Controlled. Release*, 2019, **169**, 289–295.

82 Y.-Y. Li, J. Yang, W.-B. Wu, X.-Z. Zhang and R.-X. Zhuo, *Langmuir*, 2009, **25**, 1923–1926.

83 J. Zhuang, S. Jiwpanich, V. D. Deepak and S. Thayumanavan, *ACS Macro Lett.*, 2012, **1**, 175–179.

84 Y.-C. Wang, J. Wu, Y. Li, J.-Z. Du, Y.-Y. Yuan and J. Wang, *Chem. Commun.*, 2010, **46**, 3520–3522.

85 K. Akiyoshi, S. Kobayashi, S. Shichibe, D. Mix, M. Baudys, S. W. Kim and J. Sunamoto, *J. Controlled. Release*, 1998, **5**, 313–320.

86 W. Jin, P. Xu, Y. Zhan, Y. Shen, E. A. V. Kirk, B. Alexander, W. J. Murdoch, L. Liu and D. D. Isaak, *Drug Delivery*, 2007, **14**, 279–286.

87 G. W. Ashley, J. Henise, R. Reid and D. V. Santi, *Proc. Natl. Acad. Sci. U. S. A.*, 2013, **110**, 2318–2323.

88 T. K. Bronich, S. V. Vinogradov and A. V. Kabanov, *Nano Lett.*, 2001, **1**, 535–540.

89 J. Li and D. J. Mooney, *Nat. Rev. Mater.*, 2016, **1**, 16071.

90 T. O'shea, E. K. A. A. Aimetti, V. Yesilyurt and R. Langer, *Adv. Mater.*, 2015, **27**, 65–72.

91 B. Sung, M.-H. Kim and L. Abelmann, *Bioeng. Transl. Med.*, 2021, **6**, e10190.

92 M. C. Koetting, J. T. Peters, S. D. Steichen and N. A. Peppas, *Mater. Sci. Eng., R*, 2015, **95**, 1–49.

93 M. Karimi, P. S. Zangabad, A. Ghasemi, M. Amiri, M. Bahrami, H. Malekzad, H. G. Asl, Z. Mahdieh, M. Bozorgomid, A. Ghasemi, M. R. R. T. Boyuk and M. R. Hamblin, *ACS Appl. Mater. Interfaces*, 2016, **8**, 21107–21133.

94 N. Badi, *Prog. Polym. Sci.*, 2017, **66**, 54–79.

95 S. Indulekha, P. Arunkumar, D. Bahadur and R. Srivastava, *Colloids Surf., B*, 2017, **155**, 304–313.

96 S. J. Lue, C.-H. Chen and C.-M. Shih, *J. Macromol. Sci., Part B: Phys.*, 2011, **50**, 563–579.

97 L. Yu, T. Ci, S. Zhou, W. Zeng and J. Ding, *Biomater. Sci.*, 2013, **1**, 411–420.

98 S. Han, M. Hagiwara and T. Ishizone, *Macromolecules*, 2003, **36**, 8312–8319.

99 A. A. Petryk, A. J. Giustini, R. E. Gottesman, P. A. Kaufman and P. J. Hoopess, *Int. J. Hyperthermia*, 2013, **29**, 845–851.

100 Q. Cui, S. Zhu, Y. Yan, Q. Ye, U. Ziener and Z. Cao, *J. Nanosci. Nanotechnol.*, 2015, **15**, 1533–4880.

101 D. Müller-Schulte and T. Schmitz-Rode, *J. Magn. Magn. Mater.*, 2006, **301**, 267–271.

102 V. M. Vijayan, A. E. Beeran, S. J. Shenoy, J. Muthu and V. Thomas, *ACS Appl. Bio Mater.*, 2019, **2**, 757–768.

103 J. Zhang, S. Xu and E. Kumacheva, *J. Am. Chem. Soc.*, 2004, **126**, 7908–7914.

104 B. Brugger and W. Richtering, *Adv. Mater.*, 2007, **19**, 2973–2978.

105 M. Hayati, G. R. Bardajee, M. Ramezani, S. S. Hosseini and F. Mizani, *Polym. Int.*, 2020, **69**, 156–164.

106 W.-H. Chiang, V. T. Ho, H.-H. Chen, W.-C. Huang, Y.-F. Huang, S.-C. Lin, C.-S. Chern and H.-C. Chiu, *Langmuir*, 2013, **29**, 6434–6443.

107 A. Pikabea and J. Forcada, *J. Polym. Sci., Part A: Polym. Chem.*, 2017, **55**, 3573–3586.

108 F. Gao, X. Wu, D. Wu, J. Yu, J. Yao, Q. Qi, Z. Cao, Q. Cui and Y. Mi, *Colloids Surf., A*, 2020, **587**, 124363.

109 S. Kurzhals, R. Zirbs and E. Reimhult, *ACS Appl. Mater. Interfaces*, 2015, **7**, 19342–19352.

110 J. Xie, C. Xu, N. Kohler, Y. Hou and S. Sun, *Adv. Mater.*, 2007, **19**, 3163–3166.

111 C. Lu, L. R. Bhatt, H. Y. Jun, S. H. Parkc and K. Y. Chai, *J. Mater. Chem.*, 2012, **22**, 19806–19811.

112 M. A. White, J. A. Johnson, J. T. Koberstein and N. J. Turro, *J. Am. Chem. Soc.*, 2006, **128**, 11356–11357.

113 E. Cazares-Cortes, A. Espinosa, J.-M. Guigner, A. Michel, N. Griffete, C. Wilhelm and C. Ménager, *ACS Appl. Mater. Interfaces*, 2017, **9**, 25775–25788.

114 M. Boularas, E. Gombart, J.-F. Tranchant, L. Billon and M. Save, *Rapid Commun.*, 2015, **36**, 79–83.

115 S. F. Medeiros, J. O. Filizzola, V. F. Fonseca, P. F. Oliveira, T. M. Silva, A. Elaissari and A. M. Santos, *Mater. Lett.*, 2015, **160**, 522–525.

116 R. D. Piazza, E. da Silva Nunes, W. R. Viali, S. W. da Silva, F. H. Aragón, J. A. H. Coaquira, P. C. de Morais, R. F. C. Marques and M. J. Júnior, *Carbohydr. Polym.*, 2017, **178**, 378–385.

117 T. Chen, Z. Cao, X. Guo, J. Nie, J. Xu, Z. Fan and B. Du, *Polymer*, 2011, **52**, 172–179.

118 F.-Y. Chou, C.-M. Shih, M.-C. Tsai, W.-Y. Chiu and S. J. Lue, *Polymer*, 2012, **53**, 2839–2846.

119 A. Lapresta-Fernández, A. Salinas-Castillo and L. F. Capitán-Vallvey, *Sci. Rep.*, 2021, **11**, 3947.

120 M. Rahimi, M. Yousef, Y. Cheng, E. I. Meletis, R. C. Eberhart and K. Nguyen, *J. Nanosci. Nanotechnol.*, 2009, **9**, 4128–4134.

121 S. Sayadnia, E. Arkan, R. Jahanban-Esfahlan, S. Sayadnia and M. Jaymand, *Polym. Adv. Technol.*, 2021, **32**, 262–271.

122 S. F. Medeiros, J. O. Filizzola, P. F. Oliveira, T. M. Silva, B. R. Lara, M. V. Lopes, B. Rossi-Bergmann, A. Elaissari and A. M. Santos, *Mater. Lett.*, 2016, **175**, 296–299.

123 P. Li, A. M. Zhu, Q. L. Liu and Q. G. Zhang, *Ind. Eng. Chem. Res.*, 2008, **47**, 7700–7706.

124 N. V. Mdlovu, R.-S. Juang, M.-T. Weng, Y.-S. Lin and K.-S. Lin, *ACS Appl. Nano Mater.*, 2023, **6**, 8416–8433.

125 J. Liu, C. Detrembleur, A. Debuigne, M.-C. D. Pauw-Gillet, S. Mornet, L. V. Elst, S. Laurent, E. Duguet and C. Jérôme, *J. Mater. Chem. B*, 2014, **2**, 1009–1023.

126 L. Jiang, Q. Zhou, K. Mu, H. Xie, Y. Zhu, W. Zhu, Y. Zhao, H. Xu and X. Yang, *Biomaterials*, 2013, **30**, 7418–7428.

127 C. Yao, Y. Yuan and D. Yang, *ACS Appl. Bio Mater.*, 2018, **1**, 2012–2020.

128 V. Sundaresan, J. U. Menon, M. Rahimi, K. T. Nguyen and A. S. Wadajkar, *Int. J. Pharm.*, 2014, **446**, 1–7.

129 X. Zhang, P. Wei, Z. Wang, Y. Zhao, W. Xiao, Y. Bian, D. Liang, Q. Lin, W. Song, W. Jiang and H. Wang, *ACS Appl. Mater. Interfaces*, 2022, **14**, 15956–15969.

130 K. Hayashi, M. Nakamura, H. Miki, S. Ozaki, M. Abe, T. Matsumoto, W. Sakamoto, T. Yogo and K. Ishimura, *Theranostics*, 2014, **4**, 834–844.

131 S. Indulekha, P. Arunkumar, D. Bahadur and R. Srivastava, *Colloids Surf., B*, 2017, **155**, 304–313.

132 G. Bardajee and Z. Hooshyar, *Polym. Bull.*, 2018, **75**, 5403–5419.

133 R. Gonzalez-Rodriguez, E. Campbell and A. Naumov, *PLoS One*, 2019, **14**, e0217072.

134 S. C. Kunene, K.-S. Lin, M.-T. Weng, M. J. C. Espinoza and C.-M. Wu, *J. Ind. Eng. Chem.*, 2021, **104**, 93–105.

135 A. Riedinger, M. P. Leal, S. R. Deka, C. George, I. R. Franchini, A. Falqui, R. Cingolani and T. Pellegrino, *Nano Lett.*, 2011, **11**, 3136–3141.

136 J.-M. Shen, X.-M. Guan, X.-Y. Liu, J.-F. Lan, T. Cheng and H.-X. Zhang, *Bioconjugate Chem.*, 2012, **23**, 1010–1021.

137 Y.-Y. Liu, N.-Y. Yu, W.-D. Fang, Q.-G. Tan, R. Ji, L.-Y. Yang, S. Wei, X.-W. Zhang and A.-J. Miao, *Nat. Commun.*, 2021, **12**, 812.

138 H. Wang, J. Yi, S. Mukherjee, P. Banerjeea and S. Zhou, *Nanoscale*, 2014, **6**, 13001–13011.

139 Z. Shuting, W. Jing, A. Xianquan and Z. Yan, *Front. Bioeng. Biotechnol.*, 2022, **9**, 39008–39016.

140 H. Keshavarz, A. Khavandi, S. Alamolhoda and M. R. Naimi-Jamal, *RSC Adv.*, 2020, **10**, 39008–39016.

141 W. Pon-On, T. Tithito, W. Maneeprakorn, T. Phenrat and I.-M. Tang, *Mater. Sci. Eng., C*, 2019, **97**, 23–30.

142 L. Wang, S.-M. Lai, C.-Z. Li, H.-P. Yu, P. Venkatesan and P.-S. Lai, *Pharmaceutics*, 2022, **14**, 1000.

143 A. Monfared, A. Zamanian, I. Sharifi and M. Mozafari, *Mater. Chem. Phys.*, 2019, **26**, 44–50.

144 F. Ali, K. Neha and S. Parveen, *J. Drug Delivery Sci. Technol.*, 2023, **80**, 104118.

145 A. Narang, R.-K. Chang and M. A. Hussain, *J. Pharm. Sci.*, 2013, **102**, 3867–3882.

146 M. Fonseca, I. Jarak, F. Victor, C. Domingues, F. Veiga and A. Figueiras, *Materials*, 2024, **17**, 319.

147 C. Dominguez, A. Santos, C. Alvarez-Lorenzo, A. Concheiro, I. Jarak, F. Veiga, I. Barbosa, M. Dourado and A. Figueiras, *ACS Nano*, 2022, **16**, 9994–10041.

148 S. Hua, M. B. C. de Matos, J. M. Metselaar and G. Storm, *Front. Pharmacol.*, 2018, **9**, 1–14.

149 R. Paliwal, R. J. Babu and S. Palakurthi, *AAPS PharmSciTech*, 2014, **15**, 1527–1534.

150 M. Regenold, P. Bannigan, J. C. Evans, A. Waspe, M. J. Temple and C. Allen, *Nanomedicine*, 2022, **50**, 102484.

151 R. Hergt and S. Dutz, *J. Magn. Magn. Mater.*, 2007, **311**, 187–192.

152 W. J. Atkinson, I. A. Brezovich and D. P. Chakraborty, *IEEE Trans. Biomed. Eng.*, 1984, **31**, 70–75.

153 U. Gneveckow, A. Jordan, R. Scholz, V. Brüß, N. Waldöfner, J. Ricke, A. Feussner, B. Hildebrandt and B. R. P. Wust, *Med. Phys.*, 2004, **31**, 1444–1451.

154 A. Jordan, R. Scholz, K. Maier-Hauff, F. van Landeghem, N. Waldoefner, U. Teichgraeber, J. Pinkernelle, H. Bruhn, F. Neumann, B. Thiesen, A. von Deimling and R. Felix, *J. Neurooncol.*, 2006, **78**, 7–14.

155 J.-H. Lee, J. T. Jang, J. S. Choi, S. H. Moon, S. H. Noh, J. W. Kim, J.-G. Kim, I.-S. Kim, K. I. Park and J. Cheon, *Nat. Nanotechnol.*, 2011, **6**, 418–422.

156 S. Kossatz, R. Ludwig, H. Dharing, V. Ettelt, G. Rimkus, M. Marciello, G. Salas, V. Patel, F. J. Teran and I. Hilger, *Pharm. Res.*, 2014, **31**, 3274–3288.

157 J. Pan, Y. Xu, Q. Wu, P. Hu and J. Shi, *J. Am. Chem. Soc.*, 2021, **143**, 8116–8128.

158 C. Caizer, *Nanomaterials*, 2021, **11**, 40–60.

159 B. H. de la Parte, I. Rodrigo, J. Gutiérrez-Basoa, S. I. Correcher, C. M. Medina, J. J. Echevarría-Uraga, J. A. Garcia, F. Plazaola and I. García-Alonso, *Cancers*, 2022, **14**, 3084–3098.

160 M. K. Y. Kwok, C. C. J. Maley, A. Dworkin, S. Hattersley, P. Southern and Q. A. Pankhurst, *Appl. Phys. Lett.*, 2023, **122**, 240502–240511.